International Journal of Advanced Science and Technology
Vol.91 (2016), pp.71-90
http://dx.doi.org/10.14257/ijast.2016.91.07

# Influence of Slip and Joule Heating with Radiation on MHD Peristaltic Blood Flow with Porous Medium through a Coaxial Asymmetric Vertical Tapered Channel-Blood Flow Analysis Study

SK Abzal*[1], S. Vijaya Kumar Varma[2] and S. Ravi Kumar[3]

*[1,3]Assistant Professor, Department of Mathematics*
*NBKR Institute of Science and Technology (Autonomous)*
*Vidyanagar, SPSR Nellore, Andhra Pradesh, India*
*[2]Professor, Department of Mathematics, Sri Venkateswara University*
*Tirupati, Andhra Pradesh, India*
*[1]Abzaloct23@gmail.com, [2]svijayakumarvarma@yahoo.co.in,*
*[3]drsravikumar1979@gmail.com*

***Abstract***

*In this present paper, we investigate an analysis of slip and Joule heating with radiation on MHD peristaltic blood flow with porous medium through a coaxial asymmetric vertical tapered channel under the approximations of long wavelength and low Reynolds number. An influence of various governing parameters such as Porous parameter (Da), Magnetic field (M), Prandtl number (Pr), Eckert number ($E_c$), heat source/sink parameter (γ), Brinkman number (Br) and radiation parameter (N) were discussed and illustrated graphically through a set of figures. It is noted that the temperature distribution increases by increase in N, Da, Br and M and also we observe that the temperature distribution decreases by an increase in Pr, β and γ. It can be seen that the temperature profile is found almost parabolic in nature. We notice that the heat transfer coefficient decreases in the portion of the channel x ε [0, 0.58] and then increases in the range x ε [0.58, 1] by increase in N, Br and M and also we notice that the heat transfer coefficient gradually increases in the portion of the tapered channel x ε [0, 0.58] and then it is slowly decreases in the rest of the channel x ε [0.58, 1] by increase in Pr, β, Da and γ.*

**Keywords:** *We Joule heating, radiation, porous medium, heat source/sink parameter, MHD and tapered channel*

## 1. Introduction

Motivation about the peristalsis is due to its vast occurring in many physiological mechanisms such as passage of transport of lymph in the lymphatic vessels, food transport through esophagus and urine from kidney to bladder. Utility of such flows persuaded engineers to make use of these in many industrial applications. Cosmetic products, chyme, bile, blood, mud at low shear rate, chyme and so on are examples of non-Newtonian fluids. For a long time, blood is treated as a very important fluid. Blood circulation performs different types of removal of metabolic products and removal of carbon dioxide, function in a human body such as transport of nutrients. Since the first effort to study the fluid mechanics of peristaltic transport by Latham [1]. Parkes and Burns [2] have studied the peristaltic flow produced by sinusoidal peristaltic wave along a flexible wall of the channel under the pressure gradient. After these studies, several

ISSN: 2005-4238 IJAST

investigators Fung and Yih[3] ,Zien and Ostrach [4], Raju and Devanathan [5], Srivastava *et al.*, [6], Xiao and Damodaran[7], Elshehawey and Sobh[8], Maiti[9], Radhakrishnamacharya and Srinivasulu[10], Kalidas Das [11], Lika Hummady *et al.*, [12], Ravikumar [13, 14] and M Kothandapani *et al.*, [15] have studied peristaltic problems under various assumptions.

On the other hand, Magnetohydrodynamics is also very helpful and applicable in different magnetic drug targeting like cancer diseases etc. MHD is also applicable in various engineering problems such as liquid–metal cooling of nuclear reactors, plasma confinement, electromagnetic and continuous casting process of metals. The decrements in blood pressure may cause to reduce the flow rate of blood and also it is noticed that the blood flow is affected by the presence of magnetic field because the red blood cell is a major bio-magnetic substance. In view of the above discussion many researchers studied MHD by developing different modeling. Sinha and Misra [16] analyzed blood flow under the external applied magnetic field. Effect of a moving magnetic field on blood has been analyzed by Stud *et al.*, [17].Some pertinent studies on the present topic can be found from the list of references such as M. Kothandapani [18], S. Kh. Mekheimer [19], A. J. Chamkha [20], S. Ravikumar [21, 22, 23, 24] and therein.

In dealing with heat and mass transfer problems, we examine a phenomenon called diffusion – thermo effect (Duffor effect) in which an energy flux could be generated by the concentration gradients in addition to that generated by the temperature gradients, as well on the other hand mass fluxes could be created by heat gradients which is well-known by thermal- diffusion effect (Sort effect). Srinivas and Kothandapani [25] examined the heat transfer analysis for peristaltic flow in an asymmetric channel. Few relevant studies can be seen via attempts [26-30].Radioactive convective flows are frequently encounter in many scientific and environmental processes, such as heating and cooling of chambers, astrophysical flows, water evaporation from open reservoirs, , and solar power technology. Many researchers have investigated radioactive effects on heat transfer in nonporous and porous medium utilizing the Rosseland or other radioactive flux model. Few relevant studies can be seen via attempts such as Sanyal and Adhikari [31], Hakiem [32], Raptis [33], Bakier [34], Raptis and Perdikis [35], Rao [36], Ravikumar [37] and Prasad *et al.*, [38].

## 2. Formulation of the Problem

Consider the peristaltic transport of a viscous fluid through an asymmetric vertical tapered channel through the porous medium. Asymmetry in the flow is due to the propagation of peristaltic waves of different amplitudes and phase on the channel walls. We assume that the fluid is subject to a constant transverse magnetic field $B_0$. The flow is generated by sinusoidal wave trains propagating with steady speed c along the tapered asymmetric channel walls.

The geometry of the wall surface is defined as

$$Y = H_2 = b + m'X + d \sin\left[\frac{2\pi}{\lambda}(X - ct)\right] \tag{1}$$

$$Y = H_1 = -b - m'X - d \sin\left[\frac{2\pi}{\lambda}(X - ct) + \phi\right] \tag{2}$$

Where b is the half-width of the channel, d is the wave amplitude, $c$ is the phase speed of the wave and $m'$ $((m' \ll 1)$ is the non-uniform parameter, $\lambda$ is the wavelength, t is the time and X is the direction of wave propagation. The phase difference $\phi$ varies in the range $0 \le \phi \le \pi$, $\phi = 0$ corresponds to symmetric channel with waves out of phase and further b, d and $\phi$ satisfy the following conditions for the divergent channel at the inlet $d \cos(\frac{\phi}{2}) \leq b$.

It is assumed that the left wall of the channel is maintained at temperature $T_0$, while the right wall has temperature $T_1$.

The equations governing the motion for the present problem prescribed by

$$\frac{\partial u}{\partial x} + \frac{\partial v}{\partial y} = 0 \tag{3}$$

$$\rho\left[u\frac{\partial u}{\partial x} + v\frac{\partial u}{\partial y}\right] = -\frac{\partial p}{\partial x} + \mu\left[\frac{\partial^2 u}{\partial x^2} + \frac{\partial^2 u}{\partial y^2}\right] - \left[\sigma B_0^2\right](u+c) - \left[\frac{\mu}{k_1}\right](u+c) \tag{4}$$

$$\rho\left[u\frac{\partial v}{\partial x} + v\frac{\partial v}{\partial y}\right] = -\frac{\partial p}{\partial y} + \mu\left[\frac{\partial^2 v}{\partial x^2} + \frac{\partial^2 v}{\partial y^2}\right] - \left[\sigma B_0^2\right]v - \left[\frac{\mu}{k_1}\right]v \tag{5}$$

$$\rho C_p\left[u\frac{\partial}{\partial x} + v\frac{\partial}{\partial y}\right]T = k\left[\frac{\partial^2}{\partial x^2} + \frac{\partial^2}{\partial y^2}\right]T + Q_0 + \sigma B_0^2 u^2 - \frac{\partial q}{\partial y} \tag{6}$$

u and v are the velocity components in the corresponding coordinates, $k_1$ is the permeability of the porous medium, $\rho$ is the density of the fluid, p is the fluid pressure, $k$ is the thermal conductivity, $\mu$ is the coefficient of the viscosity, $Q_0$ is the constant heat addition/absorption, $C_p$ is the specific heat at constant pressure, $\sigma$ is the electrical conductivity and T is the temperature of the fluid.

The relative boundary conditions are

$\overline{U} = 0, \overline{T} = T_0, \ \overline{C} = C_0$ at $\overline{Y} = \overline{H_1}$

$\overline{U} = 0, \overline{T} = T_1, \ \overline{C} = C_1$ at $\overline{Y} = \overline{H_2}$

The radioactive heat flux (Cogley *et al.*, [39]) is given by

$$\frac{\partial q}{\partial y} = 4\alpha^2 (T_0 - T_1) \tag{7}$$

here $\alpha$ is the mean radiation absorption coefficient.

Introducing a wave frame (x, y) moving with velocity c away from the fixed frame (X, Y) by the transformation

$$x = X - ct,\ y = Y,\ u = U - c,\ v = V \text{ and } p(x) = P(X, t) \tag{8}$$

Introducing the following non-dimensional quantities:

$$\overline{x} = \frac{x}{\lambda} \quad \overline{y} = \frac{y}{b} \quad \overline{t} = \frac{ct}{\lambda} \quad \overline{u} = \frac{u}{c} \quad \overline{v} = \frac{v}{c\delta} \quad h_1 = \frac{H_1}{b} \quad h_2 = \frac{H_2}{b} \quad p = \frac{b^2 p}{c\lambda\mu} \quad \theta = \frac{T - T_0}{T_1 - T_0}$$

$$\delta = \frac{b}{\lambda} \quad \mathrm{Re} = \frac{\rho c b}{\mu} \quad M = B_0 b\sqrt{\frac{\sigma}{\mu}} \quad \Pr = \frac{\mu C_p}{k} \quad E_c = \frac{c^2}{C_p(T_1 - T_0)} \quad \gamma = \frac{Q_0 b^2}{\mu C_p (T_1 - T_0)}$$

$$N^2 = \frac{4\alpha^2 d_1^2}{k} \quad \varepsilon = \frac{d}{b} \tag{9}$$

where $\varepsilon = \dfrac{d}{b}$ is the non-dimensional amplitude of channel , $\delta = \dfrac{b}{\lambda}$ is the wave number, $k_1 = \dfrac{\lambda m'}{b}$ is the non - uniform parameter , Re is the Reynolds number, M is the Hartman number , $K = \dfrac{k}{b^2}$ Permeability parameter ,Pr is the Prandtl number, $E_c$ is the Eckert number, $\gamma$ is the heat source/sink parameter, $B_r$ ( = $E_cP_r$) is the Brinkman number, and $N^2$ is the radiation parameter.

## 3. Solution of the Problem

In view of the above transformations (8) and non-dimensional variables (9), equations (3-6) are reduced to the following non-dimensional form after dropping the bars,

$$\operatorname{Re}\delta\left[u\frac{\partial u}{\partial x}+v\frac{\partial u}{\partial y}\right]=\left[-\frac{\partial p}{\partial x}+\delta^2\frac{\partial^2 u}{\partial x^2}+\frac{\partial^2 u}{\partial y^2}-Au-A\right] \tag{10}$$

$$\operatorname{Re}\delta^3\left[u\frac{\partial v}{\partial x}+v\frac{\partial v}{\partial y}\right]=\left[-\frac{\partial p}{\partial y}+\delta^4\frac{\partial^2 v}{\partial x^2}+\delta^2\frac{\partial^2 v}{\partial y^2}-M^2\delta^2 v-\delta^2\frac{1}{Da}v\right] \tag{11}$$

$$\operatorname{Re}\left[\delta u\frac{\partial \theta}{\partial x}+v\delta\frac{\partial \theta}{\partial y}\right]=\frac{1}{\Pr}\left[\delta^2\frac{\partial^2\theta}{\partial x^2}+\frac{\partial^2\theta}{\partial y^2}\right]+\beta+M^2Eu^2+\frac{N^2\theta}{P_r} \tag{12}$$

Applying long wave length approximation and neglecting the wave number along with low-Reynolds numbers. Equations (10-12) become

$$\frac{\partial^2 u}{\partial y^2}-Au=\frac{\partial p}{\partial x}+A \tag{13}$$

$$\frac{\partial p}{\partial y}=0 \tag{14}$$

$$\frac{1}{\Pr}\left[\delta^2\frac{\partial^2\theta}{\partial x^2}\right]+\beta+M^2Eu^2+\frac{N^2\theta}{P_r}=0 \tag{15}$$

Where $A=\left(M^2+\dfrac{1}{Da}\right)$

The relative boundary conditions in dimensionless form are given by

$$u=-\beta\frac{\partial u}{\partial y},\ \theta=0\ at\quad y=h_1=-1-k_1x-\varepsilon\sin\left[2\pi(x-t)+\phi\right] \tag{16}$$

$$u=\beta\frac{\partial u}{\partial y},\ \theta=1\text{ at}\quad y=h_2=1+k_1x+\varepsilon\sin\left[2\pi(x-t)\right] \tag{17}$$

where $\beta$ is the non-dimensional slip velocity parameter

The solutions of velocity and temperature with subject to boundary conditions (16) and (17) are given by

$$u=c_1 Sin\ h\left[\sqrt{A}\,y\right]+c_2 Cos\ h\left[\sqrt{A}\,y\right]-D \tag{18}$$

Where

 

$$c_1 = \left( \frac{D - c_2 \left[Cos\ \ h\left[\sqrt{A}h_1\right] + \beta\sqrt{A}Sin\ \ h\left[\sqrt{A}h_1\right]\right]}{Sin\ \ h\left[\sqrt{A}h_1\right] + \beta\sqrt{A}Cos\ \ h\left[\sqrt{A}h_1\right]} \right) \qquad c_2 = \frac{D\,c_3}{c_4}$$

$$c_3 = \left( \frac{Sin\ \ h\left[\sqrt{A}h_2\right] - \beta\sqrt{A}Cos\ \ h\left[\sqrt{A}h_2\right]}{Sin\ \ h\left[\sqrt{A}h_1\right] + \beta\sqrt{A}Cos\ \ h\left[\sqrt{A}h_1\right]} \right) - 1$$

$$c_4 = \left( \frac{Cos\ \ h\left[\sqrt{A}h_1\right] + \beta\sqrt{A}Sin\ \ h\left[\sqrt{A}h_1\right]}{Sin\ \ h\left[\sqrt{A}h_1\right] + \beta\sqrt{A}Cos\ \ h\left[\sqrt{A}h_1\right]} \right)\left(Sin\ \ h\left[\sqrt{A}h_2\right] - \beta\sqrt{A}Cos\ \ h\left[\sqrt{A}h_2\right]\right) - \left(Cos\ \ h\left[\sqrt{A}h_2\right] - \beta\sqrt{A}\ \ Sin\ \ h\left[\sqrt{A}h_2\right]\right)$$

Where $B = P + A \qquad D = \frac{B}{A}$

$$\theta = b_7 Cos\ \left[N\ y\right] + b_6 Sin\ \left[N\ y\right] - \left(\frac{P_r\,\gamma}{N^2}\right) - \left(\frac{M^2 B_r b_1}{4\sqrt{A}^2 + N^2} e^{2\sqrt{A}y}\right) - \left(\frac{M^2 B_r b_2}{4\sqrt{A}^2 + N^2} e^{-2\sqrt{A}y}\right) - \left(\frac{M^2 B_r b_3}{\sqrt{A}^2 + N^2} e^{\sqrt{A}y}\right) - \left(\frac{M^2 B_r b_4}{\alpha\sqrt{A}^2 + N^2} e^{-\sqrt{A}y}\right) - \left(\frac{M^2 B_r b_5}{N^2}\right) \tag{19}$$

Where

$$b_1 = \left(\frac{c_1^2}{4} + \frac{c_2^2}{4} + \frac{c_1 c_2}{2}\right) \quad b_2 = \left(\frac{c_1^2}{4} + \frac{c_2^2}{4} - \frac{c_1 c_2}{2}\right) \quad b_3 = \left(-D\,c_1 - D\,c_2\right)$$

$$b_4 = \left(D\,c_1 - D\,c_2\right) \quad b_5 = 2\left(\frac{c_2^2}{4} - \frac{c_1^2}{4}\right) + D^2$$

$$b_6 = \left( \frac{-\cos\left[N\ h_1\right] - \left[\frac{-P_r\,\gamma}{N^2}\right]\cos\left[N\ h_2\right] + \left[\frac{-P_r\,\gamma}{N^2}\right]\cos\left[N\ h_1\right]}{Sin\ \left[N\ h_1\right]\cos\left[N\ h_2\right] - Sin\ \left[N\ h_2\right]\cos\left[N\ h_1\right]} \right) -$$

$$\frac{\left(-M^2 B_r\cos\left[N\ h_2\right]\right)\left( \begin{array}{l} \frac{b_1}{4\sqrt{A}^2 + N^2} e^{2\sqrt{A}h_1} + \frac{b_2}{4\sqrt{A}^2 + N^2} e^{-2\sqrt{A}h_1} + \\ \frac{b_3}{\sqrt{A}^2 + N^2} e^{\sqrt{A}h_1} + \frac{b_4}{\sqrt{A}^2 + N^2} e^{-\sqrt{A}h_1} + \frac{b_5}{N^2} \end{array} \right)}{Sin\ \left[N\ h_1\right]\cos\left[N\ h_2\right] - Sin\ \left[N\ h_2\right]\cos\left[N\ h_1\right]} +$$

$$\frac{\left(-M^2 B_r\cos\left[N\ h_1\right]\right)\left( \begin{array}{l} \frac{b_1}{4\sqrt{A}^2 + N^2} e^{2\sqrt{A}h_2} + \frac{b_2}{4\sqrt{A}^2 + N^2} e^{-2\sqrt{A}h_2} + \\ \frac{b_3}{\sqrt{A}^2 + N^2} e^{\sqrt{A}h_2} + \frac{b_4}{\sqrt{A}^2 + N^2} e^{-\sqrt{A}h_2} + \frac{b_5}{N^2} \end{array} \right)}{Sin\ \left[N\ h_1\right]\cos\left[N\ h_2\right] - Sin\ \left[N\ h_2\right]\cos\left[N\ h_1\right]}$$

$$b_7 = \left( \frac{-b_6 Sin\,[N\ h_1] - \left( \frac{-P_r\,\gamma}{N^2} \right)}{\cos\,[N\ h_1]} \right) - \frac{\left( -M^2 B_r \left( \begin{array}{l} \frac{b_1}{4\sqrt{A}^2 + N^2} e^{2\sqrt{A}h_1} + \frac{b_2}{4\sqrt{A}^2 + N^2} e^{-2\sqrt{A}h_1} + \\ \frac{b_3}{\sqrt{A}^2 + N^2} e^{\sqrt{A}h_1} + \frac{b_4}{\sqrt{A}^2 + N^2} e^{-\sqrt{A}h_1} + \frac{b_5}{N^2} \end{array} \right) \right)}{\cos\,[N\ h_1]}$$

The coefficients of the heat transfer $Zh_1$ and $Zh_2$ at the walls $y = h_1$ and $y = h_2$ respectively, are given by

$$Zh_1 = \theta_y h_{1x} \quad (20) \qquad Zh_2 = \theta_y h_{2x} \quad (21)$$

The solutions of the coefficient of heat transfer at $y = h_1$ and $y = h_2$ are given by

$$Zh_1 = \theta_y h_{1x} = \left( -N\,b_7 Sin\,[N\ y] + Nb_6 Cos\,[N\ y] - \left( \frac{2\sqrt{A}M^2 B_r b_1}{4\sqrt{A}^2 + N^2} e^{2\sqrt{A}y} \right) - \left( \frac{-2\sqrt{A}M^2 B_r b_2}{4\sqrt{A}^2 + N^2} e^{-2\sqrt{A}y} \right) - \left( \frac{\sqrt{A}M^2 B_r b_3}{\sqrt{A}^2 + N^2} e^{\sqrt{A}y} \right) - \left( \frac{-\sqrt{A}M^2 B_r b_4}{\alpha\sqrt{A}^2 + N^2} e^{-\sqrt{A}y} \right) \right) \left( -2\pi\,\varepsilon\,Cos\,[2\pi\,(x-t)+\phi] - k_1 \right) \quad (22)$$

$$Zh_2 = \theta_y h_{2x} = \left( -N\,b_7 Sin\,[N\ y] + Nb_6 Cos\,[N\ y] - \left( \frac{2\sqrt{A}M^2 B_r b_1}{4\sqrt{A}^2 + N^2} e^{2\sqrt{A}y} \right) - \left( \frac{-2\sqrt{A}M^2 B_r b_2}{4\sqrt{A}^2 + N^2} e^{-2\sqrt{A}y} \right) - \left( \frac{\sqrt{A}M^2 B_r b_3}{\sqrt{A}^2 + N^2} e^{\sqrt{A}y} \right) - \left( \frac{-\sqrt{A}M^2 B_r b_4}{\alpha\sqrt{A}^2 + N^2} e^{-\sqrt{A}y} \right) \right) \left( 2\pi\varepsilon\ Cos\,[2\pi(-t+x)] + k_1 \right) \quad (23)$$

The volumetric flow rate in the wave frame is defined by

$$q = \int_{h_1}^{h_2} u\ dy = \left( \frac{c_1}{\sqrt{A}} \right) \left( Cos\ h[\sqrt{A}h_2] - Cos\ h[\sqrt{A}h_1] \right) + \frac{c_2}{\sqrt{A}} \left( Sin\ h[\sqrt{A}h_2] - Sin\ h[\sqrt{A}h_1] \right) + D(h_1 - h_2) \quad (24)$$

The pressure gradient obtained from equation (24) can be expressed as

$$\frac{dp}{dx} = \left( \frac{(qA)}{\left( \frac{a_1 - a_2}{\sqrt{A}} \right) \left( Cos\ h[\sqrt{A}h_2] - Cos\ h[\sqrt{A}h_1] \right) + \frac{a_3}{\sqrt{A}} \left( Sin\ h[\sqrt{A}h_2] - Sin\ h[\sqrt{A}h_1] \right) + (h_1 - h_2)} \right) - A \quad (25)$$

where

 

$$a_1 = \left( \frac{1}{Sin\ h\left[\sqrt{A}h_1\right] + \beta\sqrt{A}Cos\ h\left[\sqrt{A}h_1\right]} \right)$$

$$a_2 = \left( \frac{c_3\left( \frac{\left[Cos\ h\left[\sqrt{A}h_1\right] + \beta\sqrt{A}Sin\ h\left[\sqrt{A}h_1\right]\right]}{Sin\ h\left[\sqrt{A}h_1\right] + \beta\sqrt{A}Cos\ h\left[\sqrt{A}h_1\right]} \right)}{c_4} \right) \qquad a_3 = \frac{c_3}{c_4}$$

The instantaneous flux Q (x, t) in the laboratory frame is

$$Q = \int_{h_2}^{h_1} (u+1)\,dy = q - h \tag{26}$$

The average volume flow rate over one wave period (T = λ/c) of the peristaltic wave is defined as

$$\overline{Q} = \frac{1}{T}\int_0^T Q\,dt = q + 1 + d \tag{27}$$

From the equations (25) and (27), the pressure gradient can be expressed as

$$\frac{dp}{dx} = \left( \frac{(\overline{Q} - 1 - d)A}{\left(\frac{a_1 - a_2}{\sqrt{A}}\right)\left(Cos\ h\left[\sqrt{A}h_2\right] - Cos\ h\left[\sqrt{A}h_1\right]\right) + \frac{a_3}{\sqrt{A}}\left(Sin\ h\left[\sqrt{A}h_2\right] - Sin\ h\left[\sqrt{A}h_1\right]\right) + (h_1 - h_2)} \right) - A$$

## 4. Numerical Results and Discussion

The main object of this investigation has been to study an influence of slip and Joule heating with radiation on MHD peristaltic blood flow with porous medium through a coaxial asymmetric vertical tapered channel. The analytical expressions for velocity distribution, pressure gradient, and temperature and heat transfer coefficient have been derived in the previous section. The numerical and computational results are discussed through the graphical illustration. **Mathematica** software is used to find out numerical results.

Figures (1) - (5) present the variations of dp/dx for a given wave length verses x. Figure 1 shows that by increase in magnetic field M (M = 1, 2, 3), pressure gradient increases with fixed other parameters Da = 0.1, $k_1$= 0.1, t = π/4, $\phi$ = π/6, ε = 0.2, β = 0.1, $\overline{Q}$ = 0.2, d = 2.Influence of porous medium on pressure gradient as shown in Figure 2. This figure shows that the pressure gradient decreases by increase in porous medium Da (Da =0.1, 0.2, 0.3) being fixed β = 0.1, $\overline{Q}$ = 0.2, $k_1$= 0.1, t = π/4, $\phi$ = π/6, ε = 0.2, d = 2. Fig.3 represents the flow structure of the pressure gradient (dp/dx) for different values of $\overline{Q}$ ($\overline{Q}$ = 0.2, 0.3, 0.4) with fixed M = 0.1, Da = 0.1 $k_1$= 0.1, t = π/4, $\phi$ = π/6, ε = 0.2, β = 0.1, d = 2.It was observed that the pressure gradient decreases when $\overline{Q}$ increases. The effect of β on pressure gradient is displayed in Fig4.It is clear that the pressure gradient increases when increase in β and it is interested to note that when β = 0.2 the pressure gradient raises suddenly and requires the larger pressure gradient to maintain the same flux to pass through it. Fig.5 reveals the pressure gradient verses x. The pressure gradient is increases in the portion of the tapered channel xε [0, 0.5] and then decreases in rest of the channel xε [0.5, 1] with increasing the values φ (φ = 0, π/6, π/3) with fixed M = 0.1, Da = 0.1 $k_1$= 0.1, t = π/4, β = 0.1, ε = 0.2, $\overline{Q}$ = 0.2, d = 2.

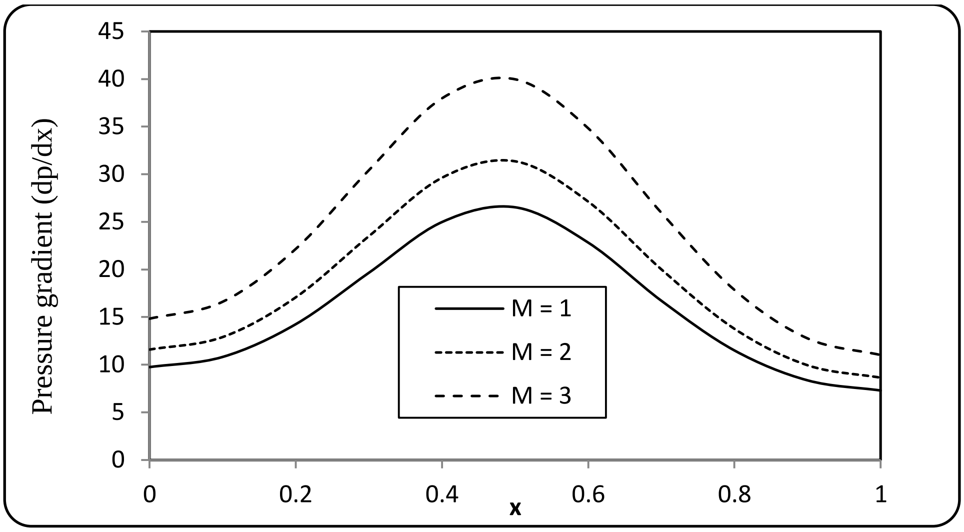


**Figure 1. Pressure Gradient (dp/dx) for Different Values of M with Fixed Da = 0.1, $k_1$= 0.1, t = π/4, $\phi$ = π/6, ε = 0.2, β = 0.1, $\overline{Q}$ = 0.2, d = 2**

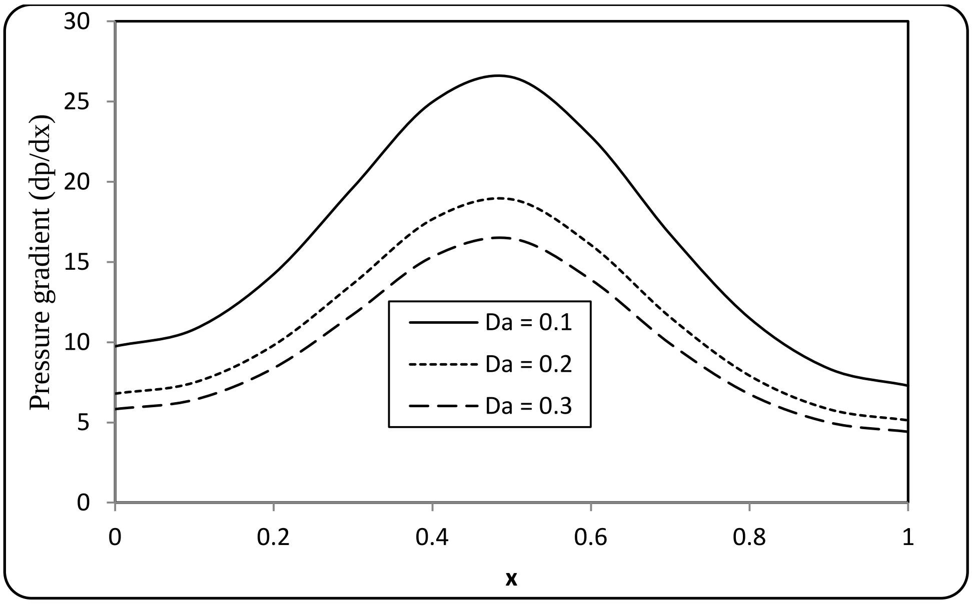


**Figure 2. Pressure Gradient (dp/dx) for Different Values of Da with β = 0.1, $\overline{Q}$ = 0.2, $k_1$= 0.1, t = π/4, $\phi$ = π/6, ε = 0.2, d = 2**

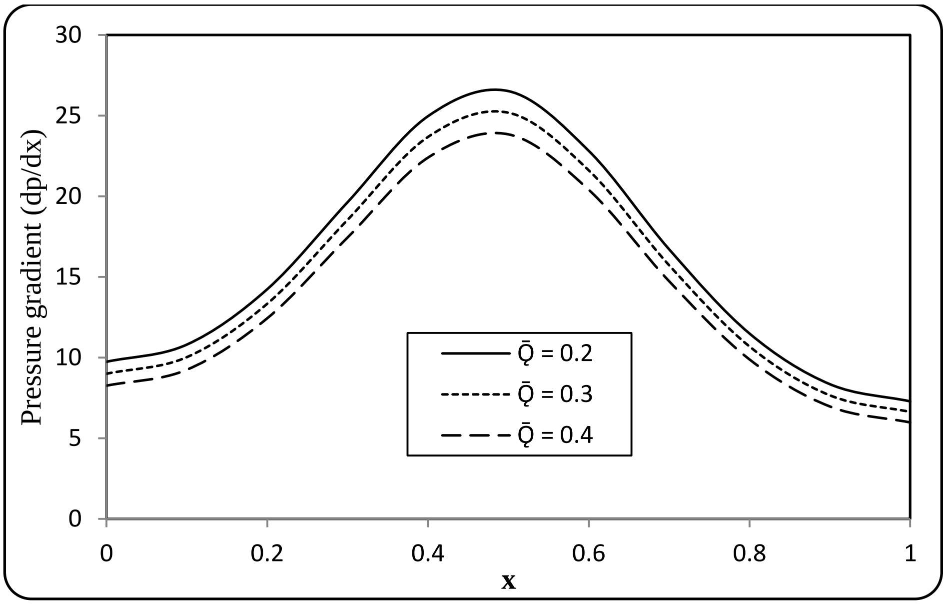


**Figure 3. Pressure Gradient (dp/dx) for Different Values of $\overline{Q}$ with Fixed M = 0.1, Da = 0.1 $k_1$= 0.1, t = π/4, $\phi$ = π/6, ε = 0.2, β = 0.1, d = 2**

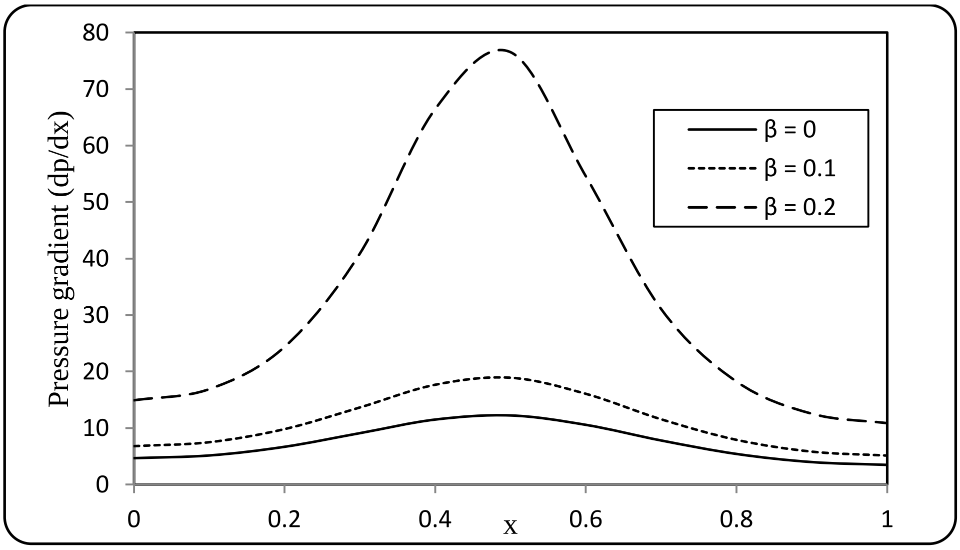


**Figure 4. Pressure Gradient (dp/dx) for Different Values of β with Fixed M = 0.1, Da = 0.1 $k_1$= 0.1, t = π/4, $\phi$ = π/6, ε = 0.2, $\overline{Q}$ = 0.2, d = 2**

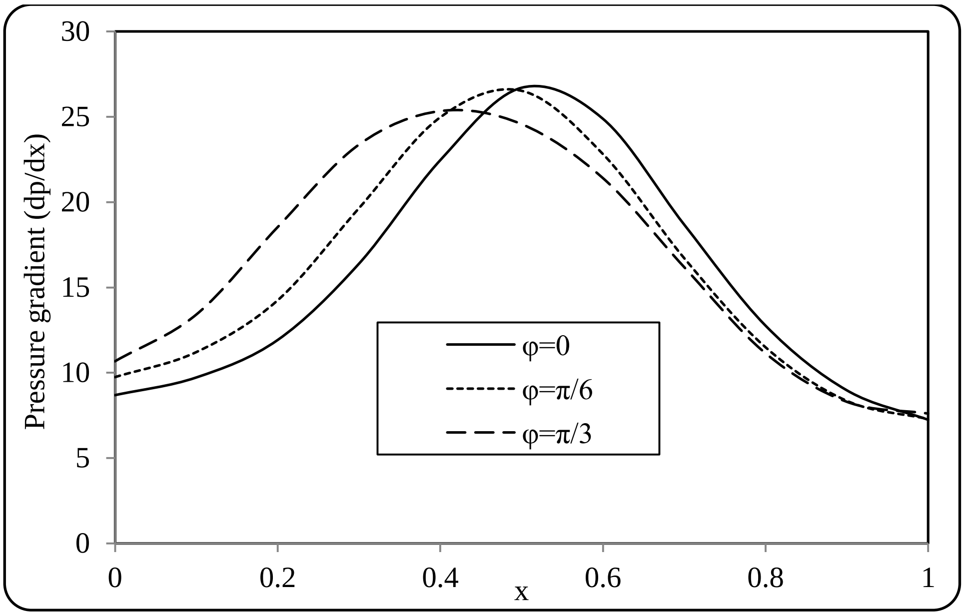


**Figure 5. Pressure Gradient (dp/dx) for Different Values of $\phi$ with Fixed M = 0.1, Da = 0.1 $k_1$= 0.1, t = π/4, β = 0.1, ε = 0.2, $\overline{Q}$ = 0.2, d = 2**

Figures 6-12 show that the effect of various parameters on temperature distribution. An influence of the radiation parameter N (N = 0.5, 0.7, 0.9) on temperature (θ) is depicted in Figure 6 with fixed Pr = 1, Br = 0.3, β = 0.5, $k_1$= 0.1, Da = 0.6, M = 1, γ = 0.1, x = 0.6, t =0. 4, ε = 0.2, $\phi$ = π/6.It is can be interpreted that the temperature increases by increase in radiation parameter N. Figure 7 reveals the temperature (θ) distribution with y. This figure reveal that the temperature distribution decreases by increasing the values of Prandtl number Pr (Pr = 1, 1.5, 2) being fixed N = 0.5, Br = 0.3, β = 0.5, $k_1$= 0.1, Da = 0.6, M = 1, γ = 0.1, x = 0.6, t =0. 4, ε = 0.2, $\phi$ = π/6. Figure 8 represents the flow structure of the temperature (θ) with different values of slip parameter (β). Indeed, the temperature slowly decreases with an increase in β (β = 0.5, 0.6, 0.7) with fixed N = 0.5, Br = 0.3, Pr = 1, $k_1$= 0.1, Da = 0.6, M = 1, γ = 0.1, x = 0.6, t =0. 4, ε = 0.2, $\phi$ = π/6. The effect of porous medium on temperature distribution (θ) is depicted in Fig.9.This figure indicates that an increase in porous parameter Da (Da = 0.1, 0.2, 0.3), results gradually increases in the temperature of the fluid with fixed N = 0.5, Br = 0.3, Pr = 1, $k_1$= 0.1, β = 0.5, M = 2, γ = 0.1, x = 0.6, t =0. 4, ε = 0.2, $\phi$ = π/6.Figure (10) presents the flow structure of the temperature (θ) with different values of Brinkman number Br (Br = 0.1, 0.3, 0.5) with fixed N = 0.5, Pr = 1, $k_1$= 0.1, β = 0.5, M = 1, Da = 0.6, γ = 0.1, x = 0.6, t =0. 4, ε = 0.2. The result gradually increases by increasing the values of brinkman number. The effect of magnetic field on temperature distribution (θ) is depicted in Figure 11. This figure reveals that the temperature distribution gradually increases by increase in magnetic field (M = 1, 2, 3) being other parameters fixed. Figure (12) reveals the temperature (θ) with heat source/sink parameter γ (γ = 0.1, 0.3, 0.5) being fixed N = 0.5, Br = 0.3, Pr = 1, $k_1$= 0.1, β = 0.5, M = 1, Da = 0.6, x = 0.6, t =0. 4, ε = 0.2, $\phi$ = π/6.The results decrease by increasing the values heat source/sink parameter γ. Hence we conclude that an increase in N, Da, Br and M, the temperature distribution increases and also we notice that the temperature distribution decreases by an increase in Pr, β and γ. We notice that the temperature profile is found almost parabolic in nature.

 

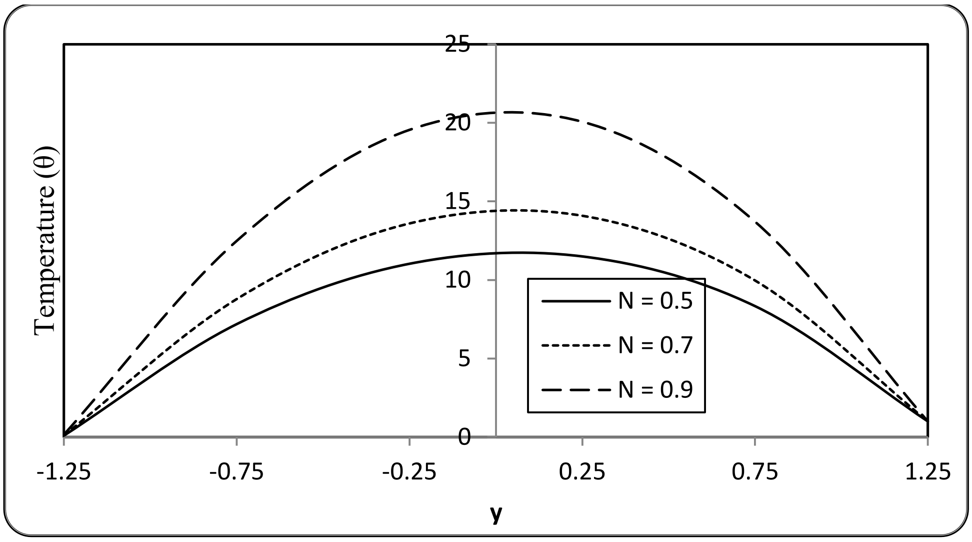


**Figure 6. Effect of N on Temperature (θ) with Fixed Pr = 1, Br = 0.3, β = 0.5, $k_1$= 0.1, Da = 0.6, M = 1, γ = 0.1, x = 0.6, t =0. 4, ε = 0.2, $\phi$ = π/6**

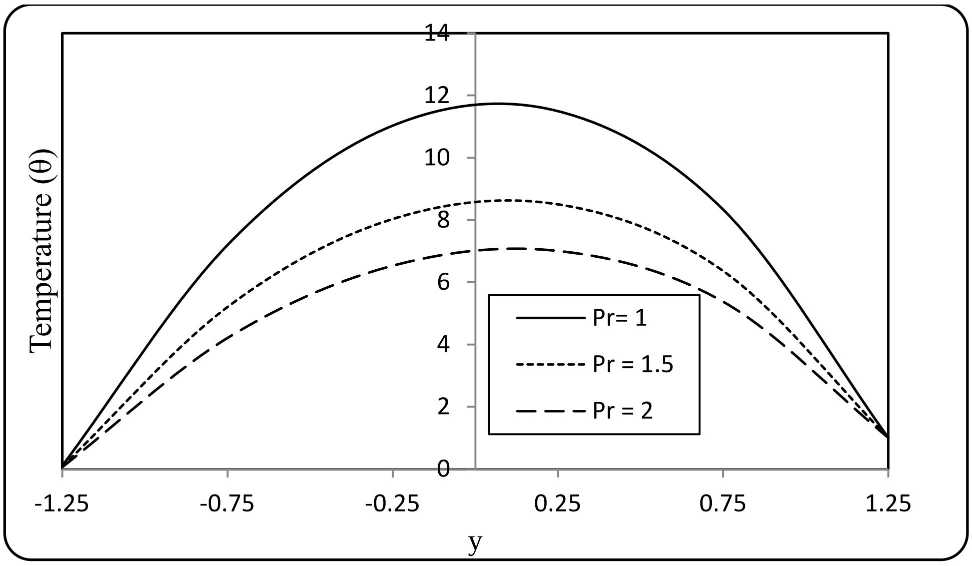


**Figure 7. Effect of Pr on Temperature (θ) with Fixed N = 0.5, Br = 0.3, β =0.5, $k_1$= 0.1, Da = 0.6, M = 1, γ = 0.1, x = 0.6, t =0. 4, ε = 0.2, $\phi$ = π/6**

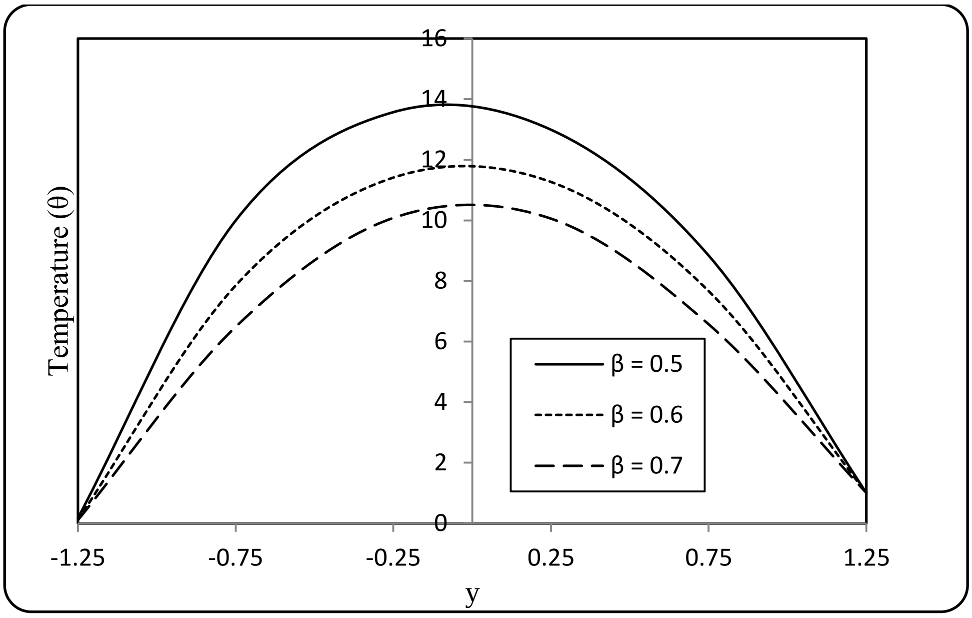


**Figure 8. Effect of β on Temperature (θ) with Fixed N = 0.5, Br = 0.3, Pr = 1, $k_1$= 0.1, Da = 0.6, M = 1, γ = 0.1, x = 0.6, t =0. 4, ε = 0.2, $\phi$ = π/6**

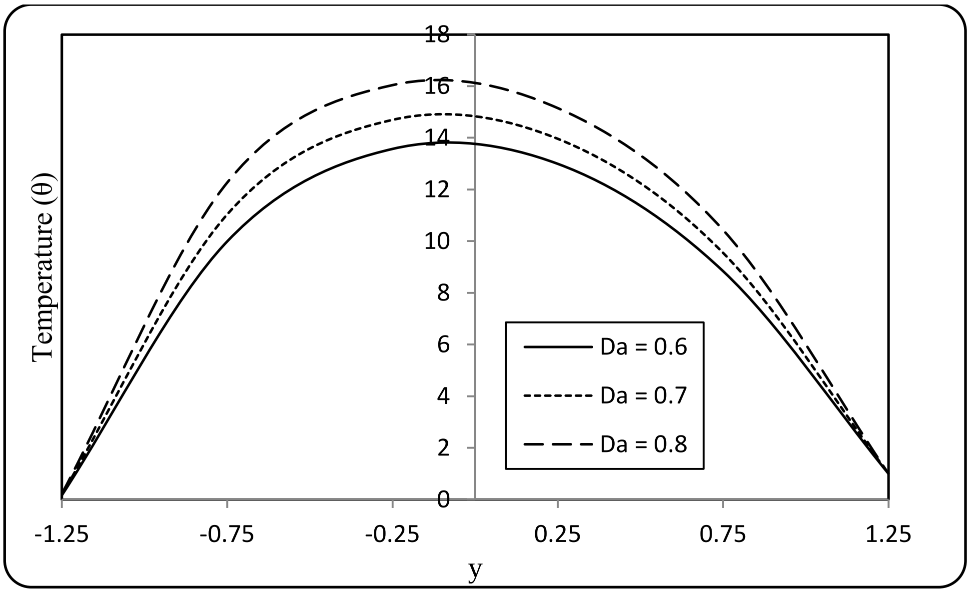


**Figure 9. Effect of Da on Temperature (θ) with Fixed N = 0.5, Br = 0.3, Pr=1, $k_1$= 0.1, β = 0.5, M = 2, γ = 0.1, x = 0.6, t =0. 4, ε = 0.2, $\phi$ = π/6**

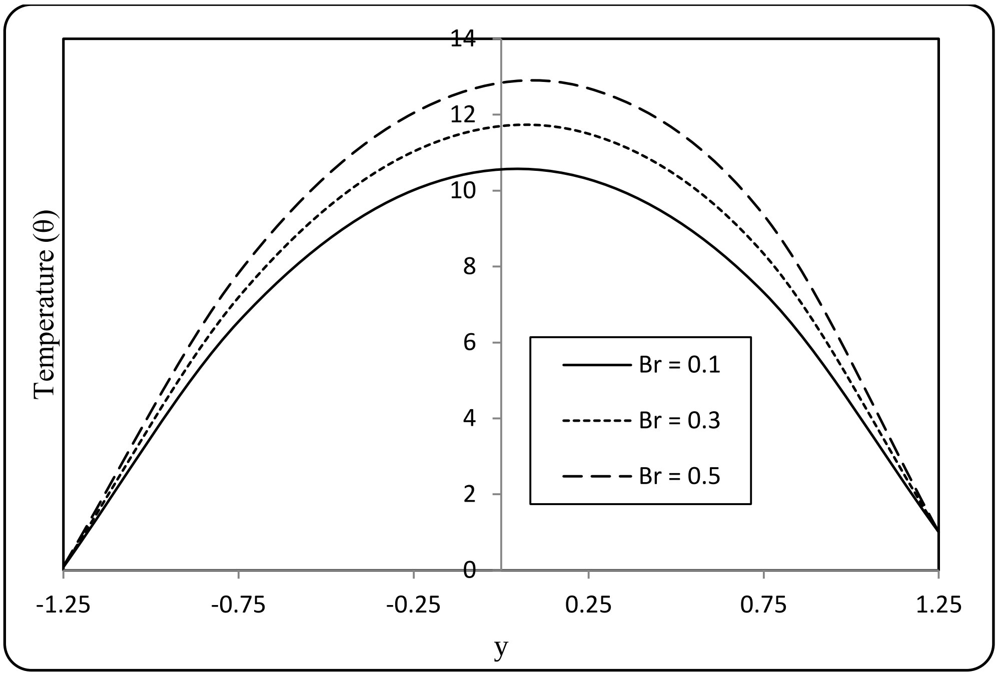


**Figure 10. Effect of Br on Temperature (θ) with Fixed N = 0.5, Pr = 1, $k_1$= 0.1, β = 0.5, M = 1, Da = 0.6, γ = 0.1, x = 0.6, t =0. 4, ε = 0.2**

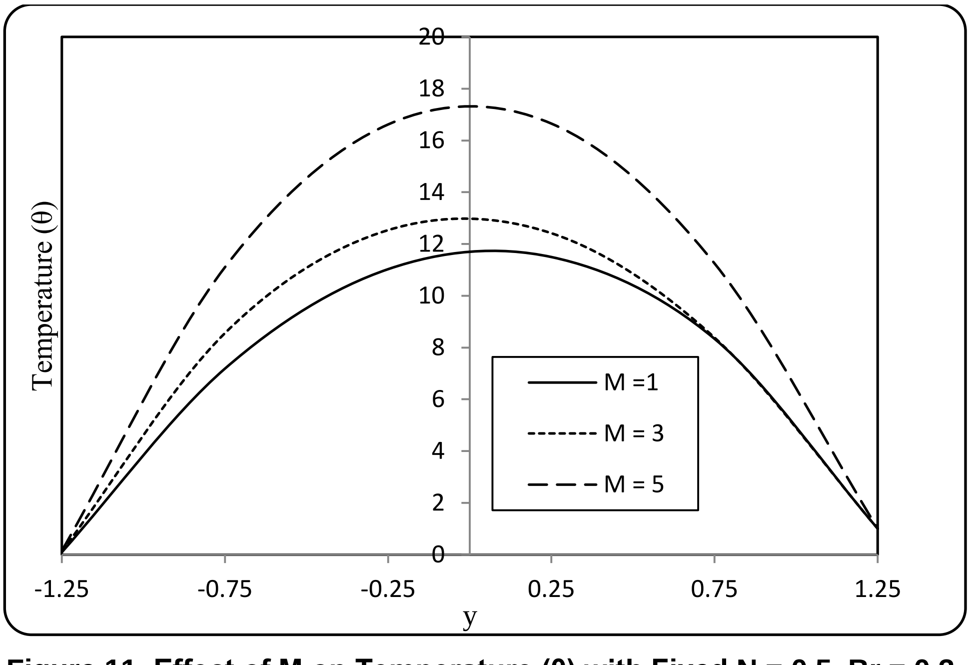


**Figure 11. Effect of M on Temperature (θ) with Fixed N = 0.5, Br = 0.3, Pr = 1, $k_1$= 0.1, β = 0.5, Da = 0.5, γ = 0.1, x = 0.6, t =0. 4, ε = 0.2, $\phi$ = π/6**

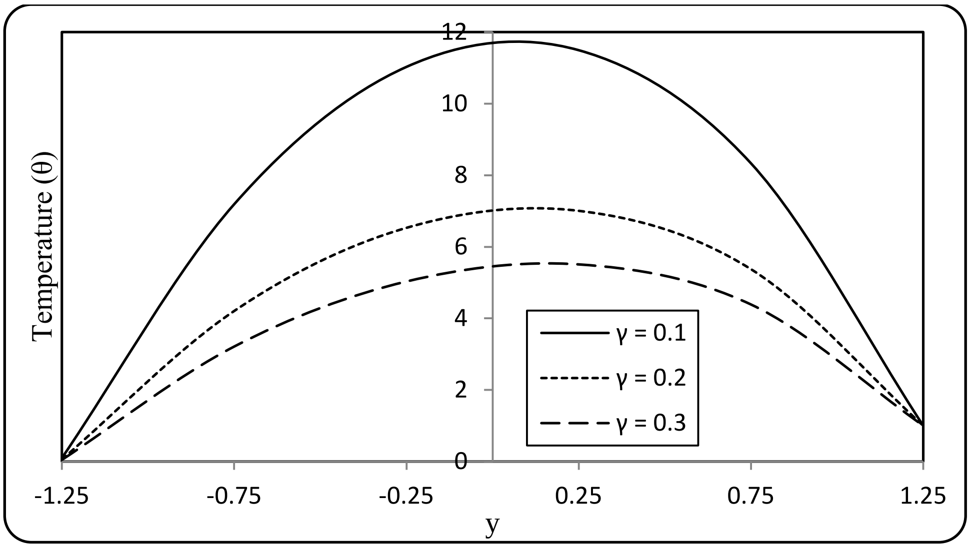


**Figure 12. Effect of γ on Temperature (θ) with fixed N = 0.5, Br = 0.3, Pr =1, $k_1$= 0.1, β = 0.5, M = 1, Da = 0.6, x = 0.6, t =0. 4, ε = 0.2, $\phi$ = π/6**

The effect of radiation parameter N on heat transfer coefficient at the wall y = $h_1$ verses x is depicted in Figure 13. Indeed, heat transfer coefficient decreases in the portion of the channel x ε [0, 0.58] and then increases in the rest of the channel x ε [0.58, 1] by increase in radiation parameter N (N = 0.5, 0.7,0.9) being fixed Br = 0.3, Pr = 1, $k_1$= 0.1, β = 0.5, Da = 0.6, γ = 0.1, M = 1, x = 0.6, t =0. 4, ε = 0.2, $\phi$ = π/6. Figure 14 shows the effect of Prandtl number on heat transfer coefficient at the wall y = $h_1$. This figure reveals that the results increases in the portion of the channel x ε [0, 0.58] and then slowly decreases in the other portion of the channel x ε [0.58, 1] with an increasing the values of Prandtl number Pr (Pr = 1, 1.5, 2) with fixed N = 0.5, Br = 0.3, $k_1$= 0.1, β = 0.5, γ = 0.1, Da = 0.6, M = 1, x = 0.6, t =0. 4, ε = 0.2, $\phi$ = π/6.Heat transfer coefficient at the wall y = $h_1$ verses x as depicted in Figure 15. The heat transfer coefficient gradually increases in the tapered channel x ε [0.58, 1] and then slowly decreases in the rest of the channel x ε [0.58, 1] by increasing the values of porous parameter Da (Da = 0.6, 0.7, 0.8) being fixed N = 0.5, Br = 0.3, $k_1$= 0.1, β = 0.5, γ = 0.1, Da = 0.6, M = 1, x = 0.6, t =0. 4, ε = 0.2, $\phi$ = π/6.Fig.16 analyzes the effect of magnetic field on heat transfer coefficient at the wall y = $h_1$ .It is found that the heat transfer coefficient decreases in x ε [0, 0.58] and then increases in x ε [0.58, 1] when M (M = 1 , 3 ,5) has higher values with N = 0.5, Br = 0.3, $k_1$= 0.1, β = 0.5, Da = 0.6, Pr = 1, γ = 0.1, x = 0.6, t =0. 4, ε = 0.2, $\phi$ = π/6. Figure 17 reveals that the heat transfer coefficient at the wall y = $h_1$ increases in the portion of the channel x ε [0, 0.58] and then decreases in the rest of the channel x ε [0.58, 1] when slip parameter β has higher values with fixed other parameters N = 0.5, Br = 0.3, $k_1$= 0.1, M = 1, Pr = 1.5, Da = 0.6, γ = 0.1, x = 0.6, t =0. 4, ε = 0.2, $\phi$ = π/6. Figure 18 presents the effect of Brinkman number Br (Br = 0.1, 0.3, 0.5) on heat transfer coefficient at y = $h_1$. We notice that the heat transfer coefficient decreases in x ε [0, 0.58] and then raises gradually in the range x ε [0.58, 1] by increasing the values of Br. Heat transfer coefficient at the wall y = $h_1$ with γ as shown in Fig.19.This figure indicates that the heat transfer coefficient increases in the portion of the tapered channel x ε [0, 0.58] and then decrease in the rest of the tapered channel x ε [0.58, 1] by increase in heat source/sink parameter γ with fixed other parameters. Finally we observe from the Figures 13-19, the heat transfer coefficient decreases in the portion of the tapered channel x ε [0, 0.58] and then raises gradually in the rest of the tapered channel x ε [0.58, 1] by increase in N, Br and M and also we notice that the heat transfer coefficient gradually increases in the channel x ε [0, 0.58] and then slowly decreases in the rest of the channel x ε [0.58, 1] by increase in Pr, β, Da and γ. We observe that the heat transfer coefficient profile is found almost an oscillatory in behaviour.

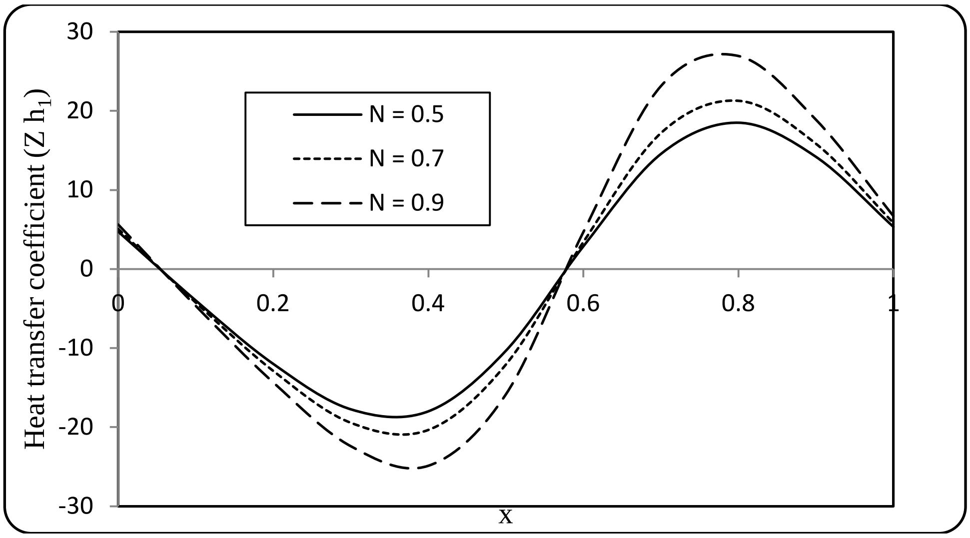


**Figure 13. Effect of N on Heat Transfer Coefficient at the Wall y = $h_1$ with Fixed Br = 0.3, Pr = 1, $k_1$= 0.1, β = 0.5, Da = 0.6, γ = 0.1, M = 1, x = 0.6, t =0. 4, ε = 0.2, $\phi$ = π/6**

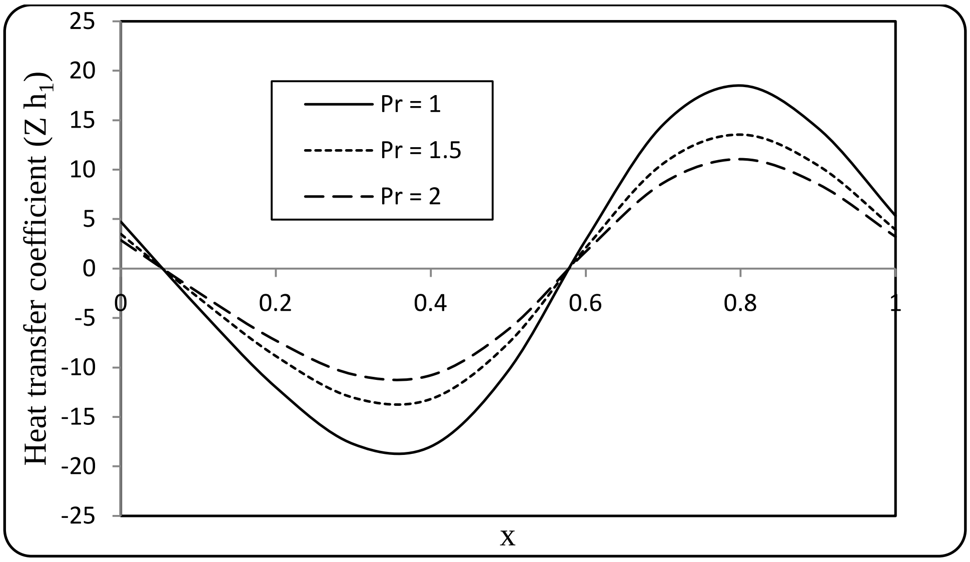


**Figure 14. Effect of Pr on Heat Transfer Coefficient at the Wall y = $h_1$ with Fixed N = 0.5, Br = 0.3, $k_1$= 0.1, β = 0.5, γ = 0.1, Da = 0.6, M = 1, x = 0.6, t =0. 4, ε = 0.2, $\phi$ = π/6**

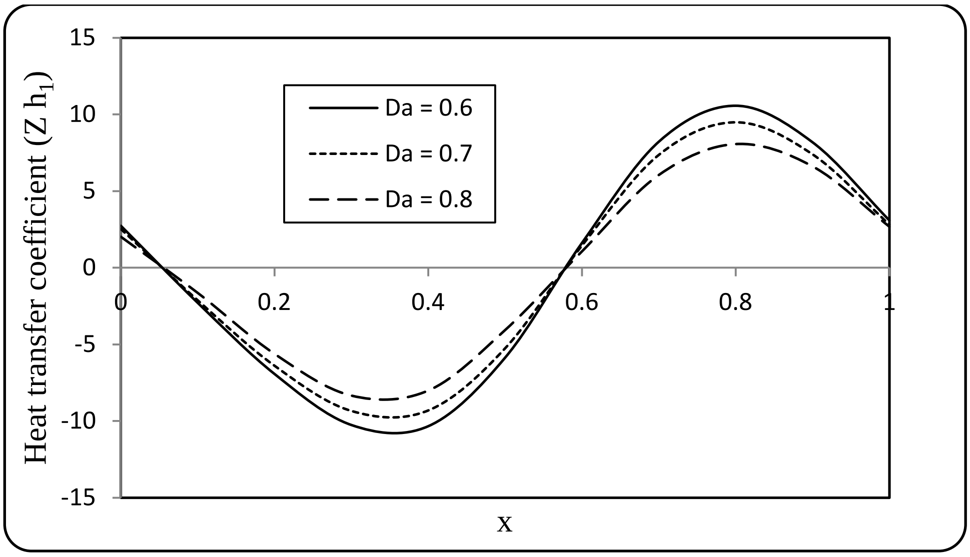


**Figure 15. Effect of Da on Heat Transfer Coefficient at the Wall $y = h_1$ with Fixed $N = 0.5$, $Br = 0.3$, $k_1 = 0.1$, $\beta = 0.5$, $Pr = 1$, $M = 1$, $\gamma = 0.1$, $x = 0.6$, $t = 0.4$, $\varepsilon = 0.2$, $\phi = \pi/6$.**

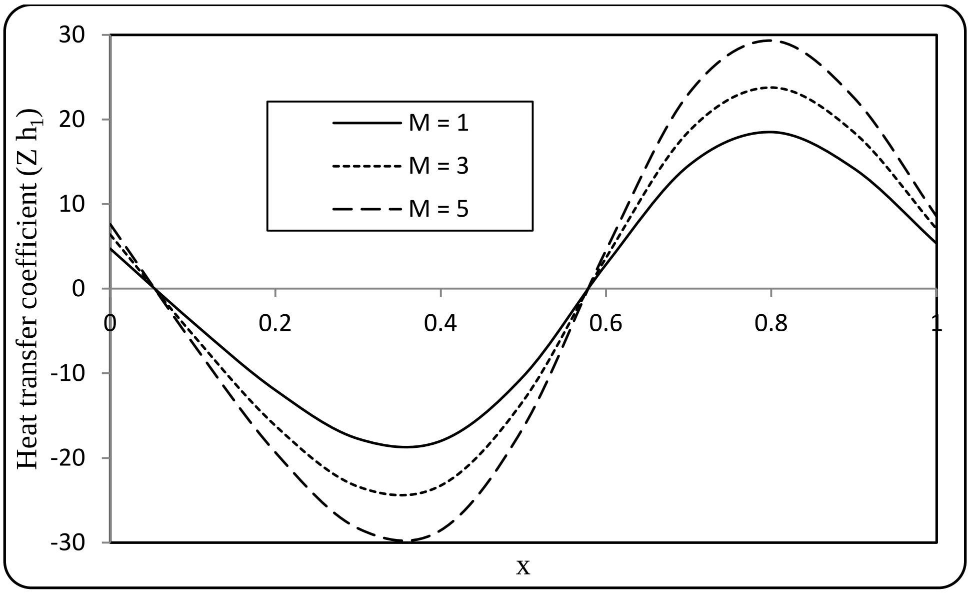


**Figure 16. Effect of M on Heat Transfer Coefficient at the Wall $y = h_1$ with Fixed $N = 0.5$, $Br = 0.3$, $k_1 = 0.1$, $\beta = 0.5$, $Da = 0.6$, $Pr = 1$, $\gamma = 0.1$, $x = 0.6$, $t = 0.4$, $\varepsilon = 0.2$, $\phi = \pi/6$.**

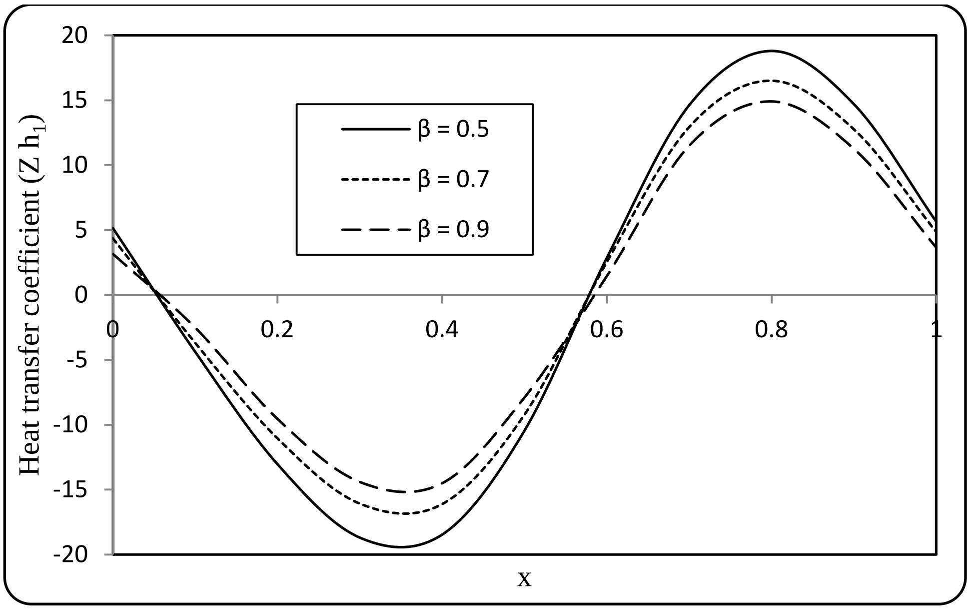


**Figure 17. Effect of β on Heat Transfer Coefficient at the Wall $y = h_1$ with Fixed N = 0.5, Br = 0.3, $k_1$= 0.1, M = 1, Pr = 1.5, Da = 0.6, γ = 0.1, x = 0.6, t =0. 4, ε = 0.2, $\phi$ = π/6**

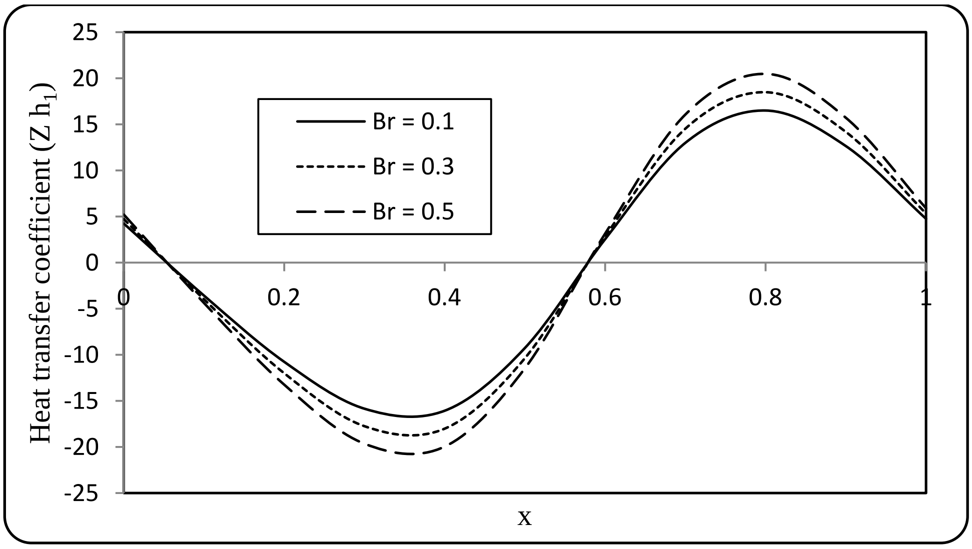


**Figure 18. Effect of Br on Heat Transfer Coefficient at the Wall $y = h_1$ with Fixed N = 0.5, Da = 0.6, $k_1$= 0.1, M = 1, Pr = 1, β = 0.5, γ = 0.1, x = 0.6, t =0. 4, ε = 0.2, $\phi$ = π/6**

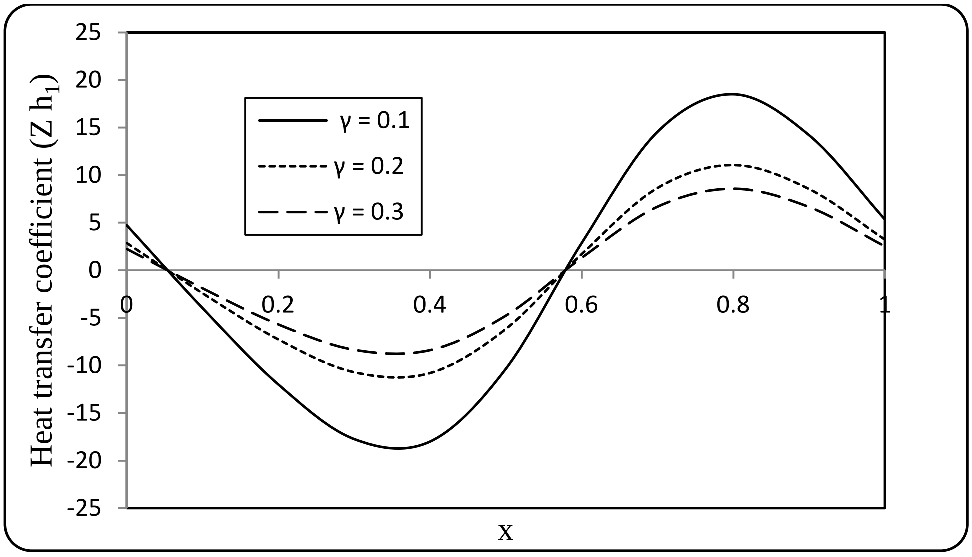


**Figure 19. Effect of γ on Heat Transfer Coefficient at the Wall $y = h_1$ with Fixed N = 0.5, Br = 0.3, $k_1$= 0.1, M = 1, Pr = 1, β = 0.5, Da = 0.6, x = 0.6, t =0. 4, ε = 0.2, $\phi$ = π/6**

## 5. Conclusions

In this present paper, a theoretical approach has been made to study the effects of an influence of slip and Joule heating with radiation on MHD peristaltic blood flow with porous medium through a coaxial asymmetric vertical tapered channel. The main observations found from the present study are given as follows.

(a) The pressure gradient increases when magnetic field M and slip parameter increased.
(b) The pressure gradient decreases when porous parameter Da and $\overline{Q}$ increased.
(c) The temperature distribution increases with increase in N, Da, Br and M.
(d) The temperature distribution decreases when Pr, β and γ increased.
(e) An increase in N, Br and M, the heat transfer coefficient decreases in the entire tapered channel.
(f) An increase in Pr, β, Da and γ, the heat transfer coefficient increases in the entire tapered channel.

## References

[1] T. W. Latham, "Fluid motion in a peristaltic pump", M S.Thesis, Massachusetts Institute of Technology, Cambridge, **(1969)**.
[2] J. Parkes and J. C. Burns, **(1967)**, "Peristaltic motion", Journal of Fluid Mechanics, vol. 29, **(1967)**, pp. 731-743.
[3] Y. C. Fung and C. S. Yih, "Peristaltic transport", Journal of Appl. Mech., Trans. ASME, vol. 5, **(1968)**, pp. 669-675.
[4] T. F. Zien and S. A. Ostrach, "Long wave length approximation to peristaltic motion", Journal of Biomech, vol. 3, **(1970)**, pp. 63.
[5] K. K. Raju and R. Devanathan, "Peristaltic motion of a non-Newtonian fluid", Rheol. Acta, vol. 11, **(1972)**, pp. 170-179.
[6] L. M. Srivastava, V. P. Srivastava and N. S. Sinha, "Peristaltic transport of a physiological fluid, Part I, Flow in non-uniform geometry", Biorheology, vol. 29, **(1983)**, pp. 153-166.
[7] Q. Xiao and M. Damodaran, "A numerical investigation of peristaltic waves in circular tubes", International Journal of Comput. Fluid Dyn., vol. 16, **(2002)**, pp. 201-216.
[8] E. F. Elsehawey and A. M. Sobh, "Peristaltic Viscoelastic Fluid Motion in a Tube", International Journal of Math.and Math, Sci., vol. 26, **(2001)**, pp. 21-34.

 

[9] S. Maiti, "Flow and heat transfer of a couple- stress fluid sandwiched between viscous fluid layers", Canadian J. of Physics, vol. 83, no. 7, **(2005)**, pp. 705-720.

[10] G. Radhakrishnamacharya and C. Srinivasulu, "Influence of wall properties on peristaltic transport with heat transfer", Comptes Rendus mechanique, vol. 335, **(2007)**, pp. 369-373.

[11] K. Das, "Effects of Slip and Heat Transfer on MHD Peristaltic Flow in An Inclined Asymmetric Channel", Iranian Journal of Mathematical Sciences and Informatics, vol. 7, no. 2, **(2012)**, pp. 35-52.

[12] L. Hummady and A. Abdulhadi, "Influence of MHD on Peristaltic Flow of Couple-Stress Fluid Through a Porous Medium with Slip Effect", Advances in Physics Theories and Applications, vol. 30, **(2014)**, pp. 34-44.

[13] S. Ravikumar, "Effect of couple stress fluid flow on magnetohydrodynamic peristaltic blood flow with porous medium trough inclined channel in the presence of slip effect-Blood flow study", International Journal of Bio-Science and Bio-Technology, vol. 7, no. 5, **(2015)**, pp. 65-84.

[14] S. Ravikumar, "Effects of the couple stress fluid flow on the magnetohydrodynamic peristaltic motion with a uniform porous medium in the presence of slip effect", Jordan Journal of Mechanical and Industrial Engineering (JJMIE), vol. 9, no. 4, **(2015)**, pp. 269-278.

[15] M. Kothandapani, V. Pushparaj and J. Prakash, "Effects of Slip and Heat Transfer on the MHD Peristaltic Flow of a Jeffery Fluid through a Vertical Tapered Asymmetric Channel", Global Journal of Pure and Applied Mathematics (GJPAM), vol. 12, no. 1, **(2016)**, pp. 205-212.

[16] A. Sinha and J. C. Misra, "MHD flow of blood through a dually stenosed artery: effects of viscosity variation, variable hematocrit and velocity slip", Can. J. Chem. Eng., vol. 92, **(2014)**, pp. 23-31.

[17] V. K. Sud, G. S. Sekhon and R. K. Mishra, "Pumping action on blood by a magnetic field", Bull. Math. Biol., vol. 39, **(1977)**, pp. 385-390.

[18] M. Kothandapani and S. Srinivas, "Peristaltic transport of a Jeffrey fluid under the effect of magnetic field in an asymmetric channel", International Journal of Nonlinear Mech., vol. 43, **(2008)**, pp. 915-924.

[19] S. Kh. Mekheimer, "Peristaltic flow of blood under the effect of magnetic field in a non uniform channel", Appl. Math. Comput., vol. 153, **(2004)**, pp. 763-777.

[20] A. J. Chamkha, "Unsteady MHD convective heat and mass transfer past a semi-infinite vertical permeable moving plate with heat absorption", International Journal of Engineering Sciences, vol. 38, **(2004)**, pp. 217-230.

[21] S. Ravikumar, "Peristaltic Fluid Flow Through Magnetic Field At Low Reynolds Number In A Flexible Channel Under An Oscilatory Flux", International journal of Mathematical Archive, vol. 4, no. 1, **(2013)**, pp. 36-52.

[22] S. Ravikumar and A. Ahmed, "Magnetohydrodynamic couple Stress Peristaltic flow of blood Through Porous medium in a Flexible Channel at low Reynolds number", Online International Interdisciplinary Research Journal, vol. III, no. VI, **(2013)**, pp. 157-166.

[23] S. Ravikumar, "Peristaltic transportation with effect of magnetic field in a flexible channel under an oscillatory flux", Journal of Global Research in Mathematical Archives, vol. 1, no. 5, **(2013)**, pp. 53-62.

[24] S. Ravikumar, "Peristaltic flow of blood through coaxial vertical channel with effect of magnetic field: Blood flow study", International Journal of Recent advances in Mechanical Engineering (IJMECH), vol. 3, no. 4, **(2014)**, pp. 85-96.

[25] S. Srinivas and M. Kothandapani, "Peristaltic transport in an asymmetric channel with heat transfer - A note", International Communication in Heat and Mass Transfer, vol. 35, **(2008)**, pp. 514-522.

[26] S. Kh. Mekheimer and Y. Abd elmaboud, "The influence of heat transfer and magnetic field on peristaltic transport of a Newtonian fluid in a vertical annulus: Application of an endoscope", Phys. Letters A, vol. 372, **(2008)**, pp. 1657-1665.

[27] K. M. Kabir, M. A. Alim and L. S. Andallah, "Effects of stress work on MHD natural convection flow along a vertical wavy surface with Joule heating", Journal of Applied Fluid Mechanics, vol. 8, **(2015)**, pp. 213-221.

[28] M. Kothandapani and S. Srinivas, "On the influence of wall properties in the MHD peristaltic transport with heat transfer and porous medium", Physics Letters A, vol. 372, **(2008)**, pp. 4586-4591.

[29] J. I. Oahimire and B. I. Olajuwon, "Effect of Hall current and thermal radiation on heat and mass transfer of a chemically reacting MHD flow of a micropolar fluid through a porous medium", Journal of King Saud University – Engineering Sciences, vol. 26, **(2014)**, pp. 112-121.

[30] M. Kothandapani and J. Prakash, "Effect of Radiation and Magnetic field on Peristaltic Transport of Nanofluids through a Porous Space in a Tapered asymmetric channel", Journal of Magn. Magn. Mater., vol. 378, **(2015)**, pp. 152-163.

[31] D. C. Sanyal and A. Adhikari, "Effects of radiation on MHD vertical channel flow", Bull. Cal. Math. Soc., vol. 98, no. 5, **(2006)**, pp. 487-497.

[32] EI. M. A. Hakiem, "MHD oscillatory flow on free convection radiation through a porous medium with constant suction velocity", Journal of Magnetism and Magnetic Materials, vol. 220, **(2000)**, pp. 271-276.

[33] A. Raptis, "Radiation and flow through a porous medium", Journal of Porous Media, vol. 4, **(2001)**, pp. 271-273.

[34] A. Y. Bakier, "Thermal radiation effects on mixed convection from vertical surfaces in saturated porous media", International Comm. Heat and Mass Transfer, vol. 28, **(2001)**, pp. 243-248.

[35] A. Raptis and C. Perdikis, "Unsteady flow through a highly porous medium in the presence of radiation", Transport in Porous Media, vol. 57, (2004), pp.171-179.
[36] C. G. Rao, "Interaction of surface radiation with conduction and convection from a vertical channel with multiple discrete heat sources in the left wall", Numer. Heat Transfer Part A: Appl., vol. 52, **(2007)**, pp. 831-848.
[37] S. Ravikumar, "Analysis of Heat Transfer on MHD Peristaltic Blood Flow with Porous Medium through Coaxial Vertical Tapered Asymmetric Channel with Radiation – Blood Flow Study", International Journal of Bio-Science and Bio-Technology, (http://dx.doi.org/10.14257/ijbsbt.2016.8.2.37), vol. 8, no. 2, **(2016)**, pp. 395-408.
[38] V. R. Prasad and N. B. Reddy, "Radiation effects on an unsteady MHD convective heat and mass transfer flow past a semi-infinite vertical permeable moving plate embedded in a porous medium", Journal of Energy, Heat and Mass Transfer, vol. 30, **(2008)**, pp. 57-78.
[39] A. C. L. Cogley, W. G. Vinvent and E. S. Giles, "Differential approximation for radiative heat transfer in non-linear equations-grey gas near equilibrium", American Institute of Aeronautics and Astronautics, vol. 6, **(1968)**, pp. 551-553.